

Function-valued RKHS-based Operator Learning for Differential Equations

Kaijun Bao^a, Xu Qian^{a,*}, Ziyuan Liu^a, Haifeng Wang^a, Songhe Song^{a,b}

^a*Department of Mathematics, College of Liberal Arts and Science, National University of Defense Technology, Changsha 410073, P.R.China*

^b*State Key Laboratory of High Performance Computing, National University of Defense Technology, Changsha 410073, China*

Abstract

Recently, a stream of works seek for solving a family of partial differential equations(PDEs), which consider solving PDEs as computing the inverse operator map between the input and solution space. Toward this end, we incorporate function-valued reproducing kernel Hilbert spaces(function-valued RKHS) into our operator learning model, which shows that the approximate solution of target operator has a special form given by the representer theorem. With an appropriate kernel and growth of the data, the approximation solution will converge to the exact one. Then we propose a neural network architecture based on the special form given by the representer theorem. We perform various experiments including advection equation, KdV equation, burgers'equation, poisson equation and show that the proposed architecture has a desirable accuracy on linear and non-linear PDE even in a small amount of data. By learning the mappings between function spaces, the proposed method has the ability to find the solution of a high-resolution input after learning from lower-resolution data.

1. Introduction

Partial differential equations(PDEs) have become a powerful tool for modeling the real world, involving many important fields such as aerospace, materials, biomolecular dynamics, etc, and achieved great success from microscopic issues (quantum, molecular dynamics) to cryoscopic issues (ship engineering). Despite the success in the application of PDEs to solve real-life problems, two significant challenges remain. First, identifying/formulating the underlying PDEs appropriate for the modeling of a specific problem is difficult; Second, solving complicated non-linear PDE systems is computationally demanding.

Modeling a specific problem and determining the approximate underlying PDE usually requires a lot of prior knowledge in the field, and combine with general conservation laws, such as the law of conservation of energy, to design its predictive model. But for complex systems, the cost of acquiring prior knowledge is usually very expensive, or the system is too simple and lacks information. Second, solving large-scale nonlinear PDEs requires a lot of computing resources, which usually makes actual simulations infeasible. This is mainly reflected in the

*This work was supported by the National Key R&D Program of China (2020YFA0709800), the National Natural Science Foundation of China (No. 11901577, 11971481, 12071481), the Natural Science Foundation of Hunan (2021JJ20053, 2020JJ5652), the science and technology innovation Program of Hunan Province (No. 2021RC3082), the Defense Science Foundation of China (2021-JCJQ-JJ-0538).

*Corresponding author.

Email address: qianxu@nudt.edu.cn (Xu Qian)

traditional numerical method for solving PDEs. Since it is very difficult to solve the analytical solution of PDEs, in practical engineering applications, we are concerned about how to give the numerical value of the solution at some discrete points in the region. Classical methods include finite difference method, finite volume method, spectrum method, finite element method, etc., and they will eventually turn the problem of solving PDEs into a problem of solving linear equations. When the problem becomes complicated, we must make the numerical method accurate enough, and the discrete points to be solved must be dense enough, such as turbulence problems. Usually the distance between discrete points must reach the order of micrometers, but this will require a lot of computing resources, which makes the problem unsolvable. Secondly, if the dimension of the problem increases, we only discretize two points in each dimension (this is already quite sparse), then our total number of discrete points exponentially explode, which is also a problem that traditional numerical methods have been facing. It is the curse of dimensionality, which will also cause the problem to become unsolvable.

In recent years, there has been a steam of works using deep neural networks to solve partial differential equation. Compared with the numerical methods, it mainly shows the advantage of efficiency. One issue is to parameterize the solution of PDE with neural networks[1, 2, 3, 4, 5, 6]. Based on the automatic differentiation, we can implement the calculation of differential terms in the PDE. Then, substituting them in the PDE to constructed the loss function, the neural network can be well trained. It is worth noting that this approach is completely data-independent, because the loss function is completely constructed by the knowledge of the underlying PDE structure. The representative work of this approach is PINN[1]. Deep rize method[2] proposed by Weinan E, which constructs the loss function via the variational form of the PDE, shows the neural network has the ability to solve high-dimension problems through Monte Carlo simulation. A tricky problem, however, is that the neural network has to be retrained when the coefficients associated with the PDEs are changed. Recalling to the numerical methods, it also has this problem. Meanwhile, another terms of work focus on solving a series of PDEs. One issue is to discretize the coefficients and solutions of PDEs at a specific resolution[7, 8, 9, 10]. Based on the data, solving PDEs is transformed to learning the map between finite Euclidean space. Such an approach, obviously, depends on the discretization size and geometry of the training data, which is impossible to query solutions at new points. Another is called by the “Neural Operators[11, 12, 13, 14, 15, 16, 17, 18]”, which is the closest steam of work to the problem we investigate. DeepONets[11], which takes inputs composed of two part: coefficients f and locations x , generates the solutions u at x . Mod-net[18] and MWT[16] are based on the integral operator $T[f](x) = \int_D K(x, y)f(y)dy$ to approximate the solutions and use the neural network to model K . We can see that the neural operators method takes the locations x into account, which can solve a series of PDEs but independ on the resolutions.

Our motivation is to treat the problem of learning a PDE as an operator learning problem. For a well-posed PDE, given coefficient, boundary condition and source term, it exists a unique solution, which means the PDE can be completely represented by the operator mapping coefficients, boundary conditions or source terms to solutions. It indicates that solving PDE can be accomplished by learning from data, but do not need to know the underlying knowledge of the PDE. Function-valued reproducing kernel Hilbert spaces[19], which induced by a unique operator-valued kernel, offers a special form given by the representer theorem to approximate an operator. And the error

between the approximate solution given by this approach and the exact solution can be estimated. It indicates that with an appropriate operator-valued kernel and growth of the data, the approximate solution will converge to the exact one in a fixed rate. Then we incorporate the function-valued RKHS into our operator learning model, and show that the proposed architecture has a desirable effect on linear and non-linear PDE. Our main contributions are as follows: I) Based on the special form for approximating operator, we develop a neural network model which learns the operator map efficiently. II) We demonstrate the applicability on one-dimensional dataset of non-linear KdV equation with a high fluctuation of the input signal. III) We show that the proposed model is a mesh-independent method, which has the ability to find the solution of a high-resolution input after learning from lower-resolution data. IV) Though the proposed model is trained on a small amount of data, it generalizes well.

2. Methodology

In this section, we transform solving PDEs into learning the operator between two infinite dimensional spaces. Based on the representer theorem in function-valued reproducing kernel Hilbert spaces, we propose a neural network structure.

2.1. Problem Setting

We aim at solving PDEs in the view of approximating the operator between two infinite dimensional spaces. The PDE we consider takes the following form:

$$\begin{aligned}(\mathcal{L}_\alpha u)(x) &= f(x), & x \in D \\ u(x) &= g(x), & x \in \partial D\end{aligned}\tag{1}$$

where \mathcal{L} is differential operator and α involves terms which determine the governing equation of PDE. We assume that PDE (1) is well-posed, which means that there exists an operator mapping from the space constructed by functions α, f, g to the space constructed by solution u . However, what we actually do is to fix two terms in functions α, f, g , and the PDE can be considered as the operator mapping the remaining term to the solution. Then, we propose to solve PDE via constructing a parametric map to approximate this operator. Without loss of generality, we fix functions α, g .

Let \mathcal{G}^\dagger be the operator mapping source term f to solution u , in PDE (1), and \mathcal{G} be the parametric map which takes f and parameter $\theta \in \Theta$ as input. Θ represents some finite-dimensional parameter space. We expect there is a $\theta^\dagger \in \Theta$ so that $\mathcal{G}(\cdot, \theta^\dagger) \approx \mathcal{G}^\dagger$.

Suppose we have observations $\{f_i, u_i\}_{i=1}^n$, where $f_i \sim \mu$ is an i.i.d. sequence from the probability measure μ supported on \mathcal{F} and u_i is the corresponding solution, which belongs to the space \mathcal{U} . To determine the parameter θ^\dagger , a natural framework is to define a cost functional $C : \mathcal{U} \times \mathcal{U} \rightarrow \mathbb{R}$ and seek a minimizer of the problem:

$$\min_{\theta \in \Theta} \mathbb{E}_{f \sim \mu} [C(\mathcal{G}(f, \theta), \mathcal{G}^\dagger(f))].\tag{2}$$

To work with problem (2) numerically, we assume functions access only to point-wise evaluations. Let P_k be a k -point discretization of the domain D and assume we have observations $f_i|_{P_k}, u_i|_{P_k}$, for a finite collection of input-output pairs indexed by i . In next section, we propose a neural network based on the theory of function-valued RKHS to learn the operator \mathcal{G}^\dagger .

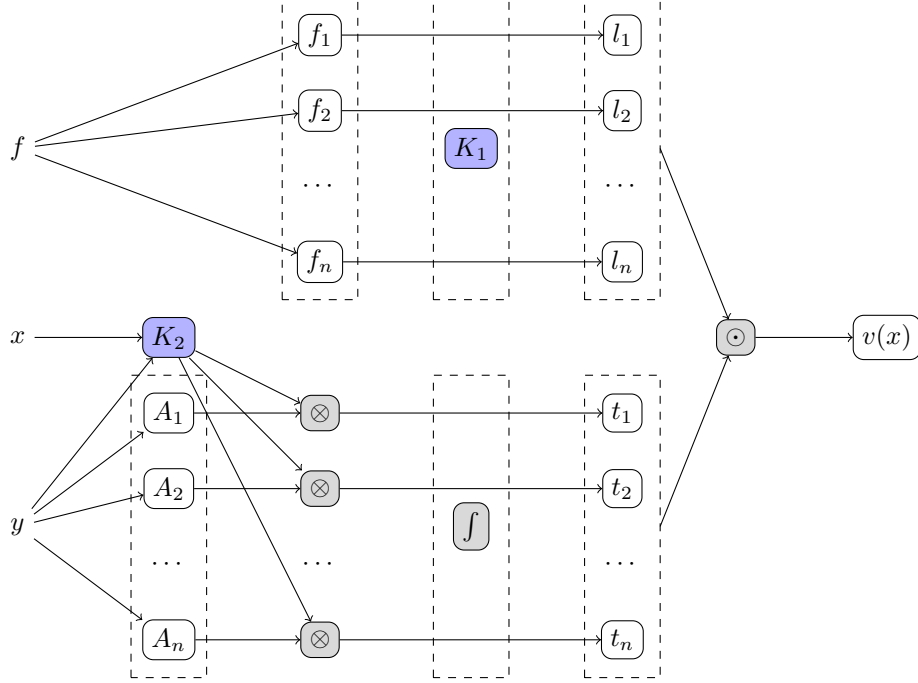


Figure 1: The architecture of function-valued RKHS-based model

2.2. Function-valued RKHS-based Model

Inspired by function-valued RKHS, which has the property that the representer theorem provides a special form for approximating an operator, and shows that it has the ability to converge to the exact operator, we propose a model based on function-valued RKHS. Above all, we consider the supervised learning in view of an operator.

Given data $\{f_i, \mathcal{G}^\dagger(f_i)\}_{i=1}^n$, we consider the following regression estimator:

$$\begin{aligned} \hat{G}_n &= \operatorname{argmin}_{G \in \mathcal{H}_k} (\hat{\mathcal{R}}_n(G) + \lambda \|G\|_{\mathcal{H}_k}^2), \\ \hat{\mathcal{R}}_n(G) &= \frac{1}{n} \sum_{i=1}^n \|G(f_i) - \mathcal{G}^\dagger(f_i)\|_{\mathcal{U}}^2, \end{aligned} \quad (3)$$

where \mathcal{H}_k is a Hilbert space about operator. Based on the data, \hat{G}_n is the optimal approximation of \mathcal{G}^\dagger . However, what we concern is if \hat{G}_n can achieve a good performance on the whole input space. The performance is characterized by the generalization error which takes the following form:

$$\mathbb{E}_{f \sim \mu} [\|\hat{G}_n(f) - \mathcal{G}^\dagger(f)\|_{\mathcal{U}}^2]. \quad (4)$$

Let $\hat{G} = \operatorname{argmin}_{G \in \mathcal{H}_k} (\mathcal{R}(G) + \lambda \|G\|_{\mathcal{H}_k}^2)$, with $\mathcal{R}(G) = \mathbb{E}_{f \sim \mu} [\|G(f) - \mathcal{G}^\dagger(f)\|_{\mathcal{U}}^2]$. Then the generalization error can be decomposed as follows:

$$\mathbb{E}_{f \sim \mu} [\|\hat{G}_n(f) - \mathcal{G}^\dagger(f)\|_{\mathcal{U}}^2] \leq \mathbb{E}_{f \sim \mu} [\|\hat{G}_n(f) - \hat{G}(f)\|_{\mathcal{U}}^2] + \mathbb{E}_{f \sim \mu} [\|\hat{G}(f) - \mathcal{G}^\dagger(f)\|_{\mathcal{U}}^2]. \quad (5)$$

Taking \mathcal{H}_k as a function-valued RKHS. It is induced by a reproducing kernel K which uniquely determines a function-valued RKHS. Following the representer theorem in function-valued RKHS, \hat{G}_n takes the following form:

$$\hat{G}_n = \sum_{i=1}^n K(f_i, \cdot) A_i, \quad (6)$$

where $A_i(\cdot)$ are in \mathcal{U} and the reproducing kernel K is a nonnegative operator-valued function. For the first term in equation (5), there has a theorem which shows that with the growth of data, $\hat{G}_n(f)$ can converge to $\hat{G}(f)$ in a fixed rate. Then, what really matters is the second term. However, it will vanish, if \mathcal{G}^\dagger belongs to the function-valued RKHS \mathcal{H}_k . Based on the discussion and equation (6), we propose the following neural network architecture.

We denote:

$$\begin{aligned} a \odot b &= [a_1 b_1, a_2 b_2, \dots, a_d b_d]^T, \\ a \otimes b &= [a_1 b_1, a_1 b_2, \dots, a_2 b_1, a_2 b_2, \dots, a_d b_1, a_d b_2, \dots]^T, \end{aligned} \quad (7)$$

where $a = [a_1, a_2, \dots, a_d]^T \in \mathbb{R}^d$ and $b = [b_1, b_2, \dots, b_d]^T \in \mathbb{R}^d$.

The whole structure of our neural network follows the encoder-decoder framework. K_1, K_2 are neural networks. They encode the input to a d -dimensional vector field and we next proceed equation (6) in the d -dimensional vector field. Finally we use a decoder to project back to the scalar field of interest.

Given data $\{f_i|_{P_k}, u_i|_{P_k}\}_{i=1}^n$ and f in PDE (1), u is the corresponding solution of f . Then we approximate u by the following steps:

$$v(x) = \sum_{i=1}^n K_1(f|_{P_k}, f_i|_{P_k}) \odot \int_D K_2(x, y) \otimes A_i(x) dy, \quad (8)$$

$$u^{app}(x) = Wv(x) + b, \quad (9)$$

with $W \in \mathbb{R}^{1 \times d}, b \in \mathbb{R}$, K_1, K_2 project the input to \mathbb{R}^d and the form of equation (8) is taken from Hilbert-Schmidt integral operator[19]. Fig.1 shows the architecture of our model.

It is worth noting that in practice, the integral in (8) can not be calculated analytically. Then we often represent it by the numerical integration. Here we use the Gauss-Chebyshev integral and our calculation process become:

$$v(x) = \sum_{i=1}^n K_1(f|_{P_k}, f_i|_{P_k}) \odot \sum_{y \in S_G} \omega_y K_2(x, y) \otimes A_i(x), \quad (10)$$

$$u^{app}(x) = Wv(x) + b, \quad (11)$$

where $S_G \subset D$ consists fixed integration points, determined by Gauss-Chebyshev integral method and ω_y are

corresponding coefficients.

In next section, we will give the experiments involving many kinds of tasks to prove the efficiency of our approach.

3. Numerical Examples

In this section, we evaluate our model on several typical PDE datasets. As mentioned in section 2, we solve the PDEs in a high resolution via traditional numerical method and obtain our training data by downsampling. The numerical results show that our method can efficiently solve PDEs based on learning the operator. Meanwhile, in training, we demonstrate that even with a small amount of training data, our model still shows good generalization properties. we also show that the proposed method exhibits mesh-independent properties, which is trained at low resolutions, but can generalize at high resolutions.

Unless stated otherwise, in our model, the architectures of neural network K_1 and K_2 are 128-256-256-128 and 128-128-128-128, with Relu activation function, and they encode inputs to a 32-dimensional vector field. K_1 is a CNN and we first use one layer to enhance the input channel to 32 without activation function. The kernel size is taken as 32 and we use padding to keep the channel unchanged. K_2 is a FNN. We choose $m = 10$ for Chebyshev polynomials and $|S_G| = 10$ in one-dimensional PDE and $|S_G| = 100$ in two-dimensional PDE for Gauss-Chebyshev integration. For all examples, we train our model in a total of 4000 epochs using Adam optimizer with an initial learning rate (LR) of 0.0002. Under applying the polynomial decay to the learning rate, we set the power of the polynomial to 0.5 and the learning rate will finally decay to 2×10^{-8} in 200 epochs. To efficiently train our model, we periodically increase the learning rate after each 200 epochs and then decrease again. Due to the structural similarity, the benchmark model we choose are recent successful neural operators. Specifically, we consider the Deep operator networks[11] (DeepONets).

The PDEs we considered include one-dimensional advection equation, burger’s equation and KdV equation and two-dimensional poisson equation. In numerical weather forecasting, it is necessary to use some excellent numerical formats to analyze the advection equation to achieve the purpose of numerical experiments and numerical prediction. Burgers’ equation is fundamental partial differential equations in various fields of applied mathematics, involving many fields of applied mathematics such as fluid mechanics, nonlinear acoustics, gas dynamics, etc. KdV equation first proposed by Dutch mathematicians Korteweg and de Vries, is used to describe nonlinear shallow water waves in fluid mechanics. Poisson equation is commonly found in electrostatics, mechanical engineering, and theoretical physics.

3.1. Advection Equation

We first consider the one-dimensional advection equation. It takes the following form:

$$\begin{aligned} \frac{\partial u}{\partial t} + \frac{\partial u}{\partial x} &= 0, x \in (0, 1), t \in (0, 1], \\ u(0, t) &= u(1, t), \end{aligned} \tag{12}$$

Our task is to use the initial conditions $u(x, 0)$ to give the solution at $u(x, t)$ at time $t=1$. In terms of data generation, we use Gaussian random fields to generate initial conditions with periodic boundary conditions, and then use numerical methods to solve the equation at high resolution, and the final training data is downsampled from the high-resolution numerical solution. The Gaussian random field is chosen $\mathcal{N}(0, 625(-\Delta + 5^2 I)^{-4})$ and we utilize chebfun package to solve the equation in 2^{11} resolution.

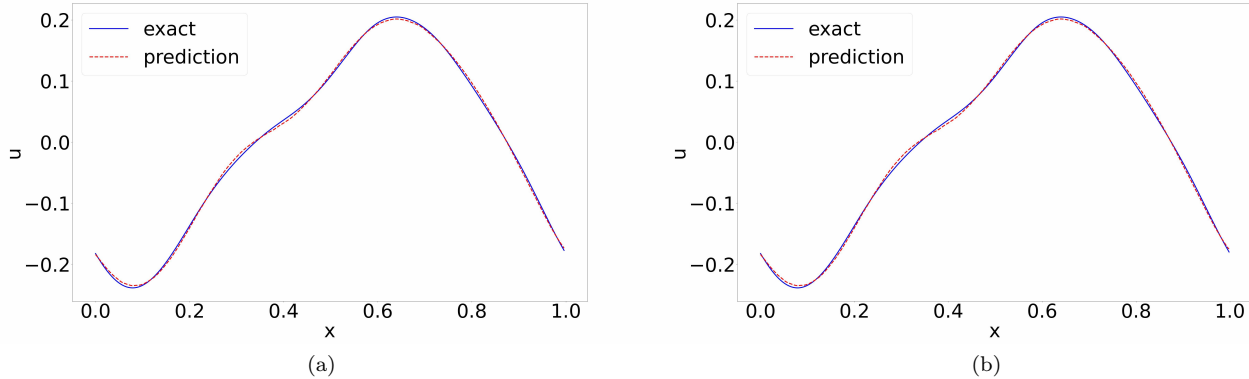


Figure 2: Advection equation: Comparison of the true solution and the learned model solution at different resolution. (a) resolution is 2^8 ; (b) resolution is 2^9 .

The experimental results of the advection equation are shown in Fig.2 and Fig.3. Fig.2 shows that given a new initial condition, we compare the approximate solution generated by our model with the exact solution in different resolution. Fig.3 shows the training error history in the view of L_2 error.

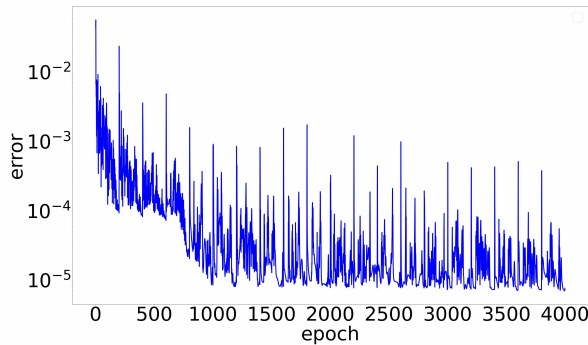


Figure 3: Advection equation: Training loss history

Our model is trained in resolution of 2^8 . The result in Fig.2 shows that the predicted solution agrees well with the exact solution and our model learned from the low resolution can evaluate at the high resolution, which shows that it correctly learn the operator about the PDE. During the training process, we see that the training loss has large fluctuations. This is because the learning rate increases periodically after each 200 epochs. Finally, our approach can achieve 1.7% relative L_2 error on the test dataset.

3.2. Burgers' Equation

The one-dimensional burgers'equation is a non-linear PDE with various applications including modeling the one dimensional flow of a viscous fluid. It takes the form

$$\begin{aligned} \frac{\partial u}{\partial t} + u \frac{\partial u}{\partial x} &= v \frac{\partial^2 u}{\partial x^2}, x \in (0, 1), t \in (0, 1], \\ u_0(x) &= u(x, t = 0), \end{aligned} \tag{13}$$

The task for the neural operator is to learn the mapping of initial condition $u(x, t = 0)$ to the solutions at $u(x, t = 1)$. The initial condition $u_0(x)$ is generated according to $u_0 \sim \mu$ where $\mu = \mathcal{N}(0, 625(-\Delta + 25I)^{-4})$ with periodic boundary conditions. We set the viscosity to $v = 0.01$ and solve the equation using a split step method where the heat equation part is solved exactly in Fourier space then the non-linear part is advanced, again in Fourier space, using a very fine forward Euler method. We solve on a spatial mesh with resolution 2^{12} and use this dataset to downsample other resolutions.

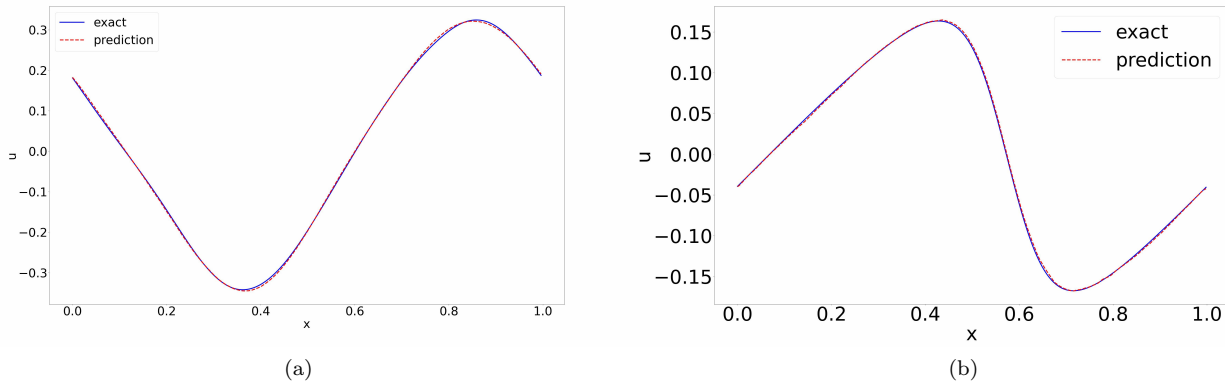


Figure 4: Burgers' equation: Comparison of the true solution and the learned model solution in two different inputs.

The results of our experiments are shown in Fig.4, Fig.5, Tab.1 and Tab.2. Fig.4 shows that given new initial conditions, we compare the approximate solution generated by our model with the exact solution. Fig.4 and Tab.1 show the comparison of our model and DeepONets in view of the relative L_2 error. Tab.2 shows the result that our model trained in some resolutions generalize at various input resolutions.

The result shows that the predicted solution produced by our approach approximate well with the exact solution, and compared to DeepONets, our approach shows a better result. Moreover, as the increasing of the resolution, we see that the relative error of DeepONets gradually increases, but our model does not. It learns better in the high resolution than the low resolution. At the same time, we see that our model shows the property of mesh-independent. When the model trained in a resolution test in different resolutions, the relative error almost does not change.

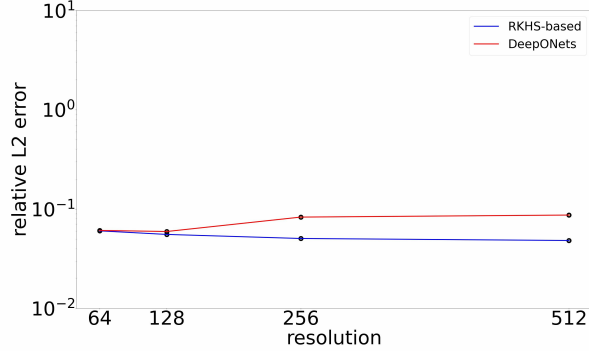


Figure 5: Burgers' equation: Burgers' equation validation at various input resolutions

Resolutions	$s = 64$	$s = 128$	$s = 256$	$s = 512$
RKHS-based	0.0604	0.0556	0.0506	0.0482
DeepONets	0.0610	0.0595	0.0831	0.0871

Table 1: Burgers' equation: Benchmarks on Burgers' equation at various input resolution

Resolutions	$s' = 64$	$s' = 128$	$s' = 256$	$s' = 512$
$s = 64$	0.0604	0.0608	0.0610	0.0611
$s = 128$	0.0557	0.0556	0.0556	0.0556
$s = 256$	0.0506	0.0505	0.0506	0.0506
$s = 512$	0.0484	0.0483	0.0484	0.0482

Table 2: Burgers' equation: Resolutions in the training and testing

3.3. Korteweg-de Vries (KdV) Equation

The one-dimensional KdV equation takes the following form

$$\begin{aligned} \frac{\partial u}{\partial t} &= -0.5u \frac{\partial u}{\partial x} - \frac{\partial^3 u}{\partial x^3} x \in (0, 1), t \in (0, 1], \\ u_0(x) &= u(x, t = 0), \end{aligned} \tag{14}$$

As mentioned above, we still solve the equation by learning the mapping of initial condition $u(x, t = 0)$ to the solutions $u(x, t)$ at $t = 1$. The initial condition $u_0(x)$ is generated according to a random field[20] with a fluctuating parameter λ and we take $\lambda = 0.25$. We solve on a spatial mesh with resolution 2^{12} and use this dataset to downsample other resolutions to train our model.

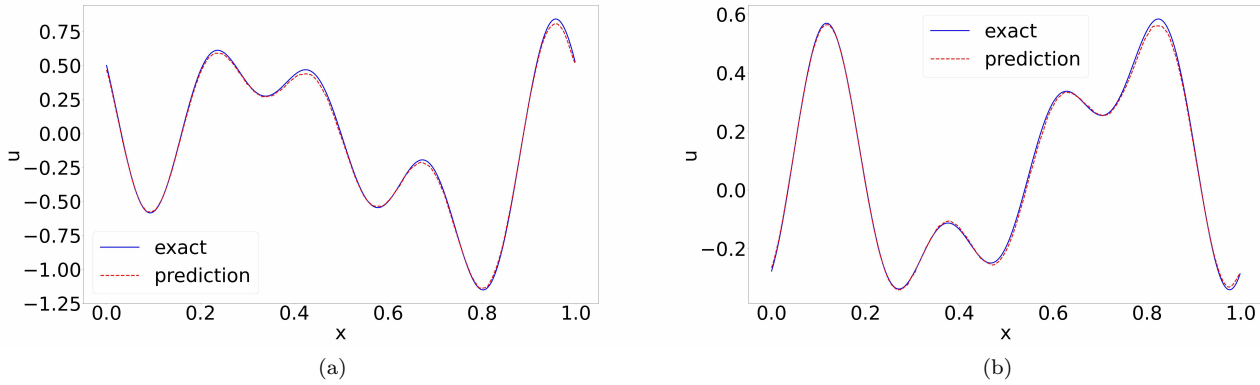


Figure 6: KdV equation: Comparison of the true solution and the learned model solution in two different inputs.

The results of our experiments are shown in Fig.6, Fig.7, Tab.3 and Tab.4. Fig.6 shows that given new initial condition, we compare the approximate solution generated by our model with the exact solution. Fig.7 and Tab.3 show the comparison of our model and DeepONets in view of the relative L_2 error. Tab.4 shows the result that our model trained in some resolutions generalize at various input resolutions.

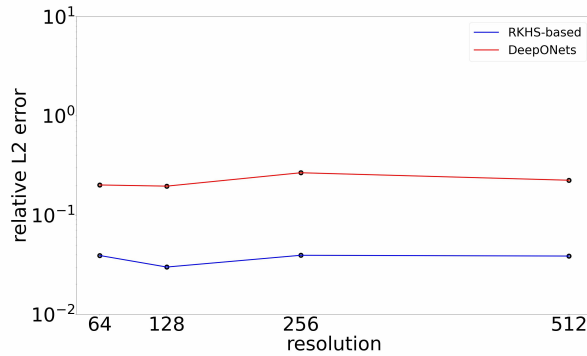


Figure 7: KdV equation: KdV equation validation at various input resolutions

It is worth noting that compared to DeepONets, our model also achieve a better relative error and compared to the experiment of burgers equation, Our approach still maintains a small relative error. the predicted solution shows a great agreement with the exact solution. While DeepONets does not perform well for large fluctuations. Meanwhile, at various input resolution, our approach can achieve the same degree of relative error and when we test the trained model at a different resolution, the relative error has little fluctuation. These show that our approach is a mesh-independent method and have the property of stability.

Resolutions	$s = 64$	$s = 128$	$s = 256$	$s = 512$
RKHS-based	0.0391	0.0300	0.0394	0.0387
DeepONets	0.2011	0.1957	0.2669	0.2244

Table 3: Kdv equation: Benchmarks on Kdv equation at various input resolution

Resolutions	$s' = 64$	$s' = 128$	$s' = 256$	$s' = 512$
$s = 64$	0.0391	0.0399	0.0404	0.0406
$s = 128$	0.0291	0.0300	0.0310	0.0315
$s = 256$	0.0396	0.0395	0.0394	0.0394
$s = 512$	0.0386	0.0388	0.0387	0.0387

Table 4: KdV equation: Resolutions in the training and testing

3.4. Poisson equation

We consider the Poisson equation[18]:

$$\begin{aligned}
 -\Delta u(x) &= f(x), x \in D, \\
 u(x) &= 0, x \in \partial D,
 \end{aligned}
 \tag{15}$$

Consider 2D case, in which source function f is generated by $-a(x^2 - x + y^2 - y)$, i.e.,

$$\begin{aligned}
 \partial_{xx}u + \partial_{yy}u &= -a(x^2 - x + y^2 - y), (x, y) \in D, \\
 u &= 0, (x, y) \in \partial D,
 \end{aligned}
 \tag{16}$$

where $D = [0, 1]^2$ and constant a controls the source term. Obviously, the analytical solution is $u = \frac{a}{2}x(x-1)y(y-1)$.

In this experiments, the settings of training process is different from that mentioned above. During training, we sample $K = 10$ source functions g from selected region, that is, we sample control parameter a uniformly from $\{10k\}_{k=1}^{20}$ and the training data we select by, for each epoch, randomly sample 200 points in $[0, 1]^2$ and sample 100 points in each line of boundary, respectively. For the input of K_1 , we take P_k as 64×64 isometric grid points. It is worth noting that, in previous experiments, the training points are also P_k . Finally, we test the performance of our well-trained model on $a = 15$. For visualizing the performance of our well-trained model, we show the exact solution and the predicted solution on 101×101 isometric grid points. To compare these two solutions more intuitively, we

calculate the difference of the two solutions at each point and show the error by color. These results are showed in Fig.8. The relative L_2 error is 1.5%.

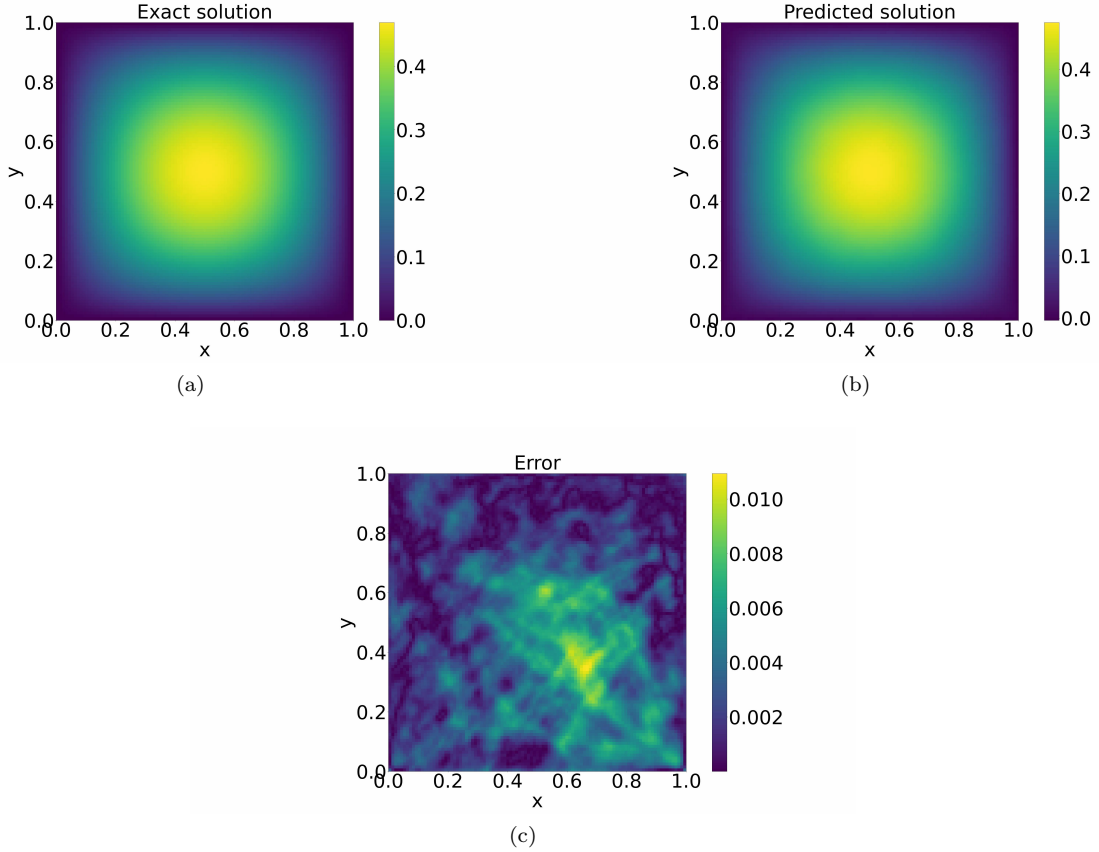


Figure 8: Poisson equation: Comparison between exact solution and predicted solution on 101×101 grid points corresponding to source terms determined by $a = 15$. (a) Exact solution. (b) Predicted solution. (c) The difference between the exact solution and predicted solution.

We also test DeepONets on two-dimensional Poisson equation. The training process is similar as us by sampling $K = 10$ source functions g from selected region and for each epoch, randomly sampling 200 points in $[0, 1]^2$ and sampling 100 points in each line of boundary, respectively. Finally, we observe that the testing relative L_2 error is 62.3%, which means that with a small amount of data, DeepONets fails learning the exact operator.

4. Conclusion

In this work, we transform the problem of solving PDEs to the problem of data-driven learning of the operator that maps between two function spaces. Motivated from the fundamental properties of the function-valued RKHS, we address this problem by proposing a neural network following the form given by the representer theorem and the kernel is constructed by Hilbert-Schmidt integral operator. We show that the proposed model have a great performance on several kind of PDEs, even the solution have a high fluctuation. Meanwhile, Numerical experiments

show that our approach is a mesh-independent method, which has the ability to find the solution of a high-resolution input after learning from lower-resolution data, and have the property of stability. Additionally, another outstanding advantage of our model is that it only uses a small amount of data to train, but has a good generalization.

References

- [1] M. Raissi, P. Perdikaris, G. E. Karniadakis, Physics-informed neural networks: A deep learning framework for solving forward and inverse problems involving nonlinear partial differential equations, *Journal of Computational physics* 378 (2019) 686–707.
- [2] B. Yu, et al., The deep ritz method: a deep learning-based numerical algorithm for solving variational problems, *Communications in Mathematics and Statistics* 6 (1) (2018) 1–12.
- [3] J. Sirignano, K. Spiliopoulos, Dgm: A deep learning algorithm for solving partial differential equations, *Journal of computational physics* 375 (2018) 1339–1364.
- [4] Y. Zang, G. Bao, X. Ye, H. Zhou, Weak adversarial networks for high-dimensional partial differential equations, *Journal of Computational Physics* 411 (2020) 109409.
- [5] S. Dong, Z. Li, Local extreme learning machines and domain decomposition for solving linear and nonlinear partial differential equations, *Computer Methods in Applied Mechanics and Engineering* 387 (2021) 114129.
- [6] J. Yu, L. Lu, X. Meng, G. E. Karniadakis, Gradient-enhanced physics-informed neural networks for forward and inverse pde problems, *arXiv preprint arXiv:2111.02801* (2021).
- [7] J. Adler, O. Öktem, Solving ill-posed inverse problems using iterative deep neural networks, *Inverse Problems* 33 (12) (2017) 124007.
- [8] S. Bhatnagar, Y. Afshar, S. Pan, K. Duraisamy, S. Kaushik, Prediction of aerodynamic flow fields using convolutional neural networks, *Computational Mechanics* 64 (2) (2019) 525–545.
- [9] X. Guo, W. Li, F. Iorio, Convolutional neural networks for steady flow approximation, in: *Proceedings of the 22nd ACM SIGKDD international conference on knowledge discovery and data mining*, 2016, pp. 481–490.
- [10] Y. Zhu, N. Zabaras, Bayesian deep convolutional encoder–decoder networks for surrogate modeling and uncertainty quantification, *Journal of Computational Physics* 366 (2018) 415–447.
- [11] L. Lu, P. Jin, G. E. Karniadakis, Deeponet: Learning nonlinear operators for identifying differential equations based on the universal approximation theorem of operators, *arXiv preprint arXiv:1910.03193* (2019).
- [12] S. Wang, H. Wang, P. Perdikaris, Learning the solution operator of parametric partial differential equations with physics-informed deeponets, *Science advances* 7 (40) (2021) eabi8605.

- [13] Z. Li, N. Kovachki, K. Azizzadenesheli, B. Liu, K. Bhattacharya, A. Stuart, A. Anandkumar, Neural operator: Graph kernel network for partial differential equations, arXiv preprint arXiv:2003.03485 (2020).
- [14] Z. Li, N. Kovachki, K. Azizzadenesheli, B. Liu, A. Stuart, K. Bhattacharya, A. Anandkumar, Multipole graph neural operator for parametric partial differential equations, *Advances in Neural Information Processing Systems* 33 (2020) 6755–6766.
- [15] Z. Li, N. Kovachki, K. Azizzadenesheli, B. Liu, K. Bhattacharya, A. Stuart, A. Anandkumar, Fourier neural operator for parametric partial differential equations, arXiv preprint arXiv:2010.08895 (2020).
- [16] G. Gupta, X. Xiao, P. Bogdan, Multiwavelet-based operator learning for differential equations, *Advances in Neural Information Processing Systems* 34 (2021).
- [17] K. Wu, D. Xiu, Data-driven deep learning of partial differential equations in modal space, *Journal of Computational Physics* 408 (2020) 109307.
- [18] L. Zhang, T. Luo, Y. Zhang, Z.-Q. J. Xu, Z. Ma, Mod-net: A machine learning approach via model-operator-data network for solving pdes, arXiv preprint arXiv:2107.03673 (2021).
- [19] H. Kadri, E. Duflos, P. Preux, S. Canu, A. Rakotomamonjy, J. Audiffren, Operator-valued kernels for learning from functional response data, *Journal of Machine Learning Research* 17 (20) (2016) 1–54.
- [20] S. Filip, A. Javeed, L. N. Trefethen, Smooth random functions, random odes, and gaussian processes, *SIAM Review* 61 (1) (2019) 185–205.